Neurobiology of Aging 79 (2019) 142–151

Contents lists available at ScienceDirect

Neurobiology of Aging

journal homepage: www.elsevier.com/locate/neuaging

Altered slow (<1 Hz) and fast (beta and gamma) neocortical oscillations in the 3xTg-AD mouse model of Alzheimer's disease under anesthesia

Patricia Castano-Prat [a], Lorena Perez-Mendez [a], Maria Perez-Zabalza [a], Coral Sanfeliu [b], Lydia Giménez-Llort [c], Maria V. Sanchez-Vives [a,d,*]

[a] Systems Neuroscience, IDIBAPS (Institut d'Investigacions Biomèdiques August Pi i Sunyer), Barcelona, Spain
[b] Biomedical Research Institute of Barcelona (IIBB), Consejo Superior de Investigaciones Científicas (CSIC), IDIBAPS and CIBERESP, Barcelona, Spain
[c] Institut de Neurociènces and Department of Psychiatry and Forensic Medicine, School of Medicine, Universitat Autònoma de Barcelona (UAB), Barcelona, Spain
[d] ICREA, Barcelona, Spain

ARTICLE INFO

Article history:
Received 11 April 2018
Received in revised form 24 January 2019
Accepted 9 February 2019
Available online 13 March 2019

Keywords:
Aging
Alzheimer disease
Gamma oscillations
Gamma rhythm
Slow oscillations
Up states
Cerebral cortex
Transgenic model
Excitability

ABSTRACT

The 3xTg-AD mouse model reproduces the main features associated with the etiology of familial Alzheimer's disease (AD). To investigate whether these features imply functional cortical network alterations and their evolution with age, we studied spontaneous slow oscillations, activity that integrates cellular and network properties. We quantified different parameters of the emergent slow oscillations—alternating Up and Down states—and of the embedded beta-gamma rhythms of 3xTg-AD and wild-type mice at 7 and 20 months of age. Most group differences occurred at 20 months of age: 3xTg-AD mice presented lower oscillatory frequency, higher cycle variability, and reduced relative (Up/Down) firing rate with respect to controls. The high-frequency analysis revealed a shift toward lower frequencies in older 3xTg-AD animals, reminiscent of one of the electroencephalography hallmarks of patients with AD. This first systematic characterization of the cortical emergent rhythms in 3xTg-AD strain provides insights into the network mechanisms underlying associated network activity alterations.

1. Introduction

Alzheimer's disease (AD) is a primary neurodegenerative disorder that causes a progressive impairment of memory and other cognitive functions, and represents the leading cause of dementia among the elderly. The principal neuropathological hallmarks of AD are the abnormal accumulation of the amyloid-β (Aβ) peptide forming Aβ plaques, the hyperphosphorylation of the microtubule-associated protein tau—known as neurofibrillary tangles—the loss of neurites and synapses, and cellular death at advanced stages of the disease (for a review, see Querfurth and LaFerla, 2010). Most of the mouse models of AD mimic only some of the aforementioned features of the disease (Wong et al., 2002). The triple-transgenic mouse model of AD (3xTg-AD), on the other hand, develops Aβ and tau pathology in a progressive, temporal- and region-specific manner that resembles that in human AD brain (LaFerla and Oddo, 2005; Oddo et al., 2003a,b). At 7 months of age, 3xTg-AD mice present intracellular Aβ immunoreactivity in the neocortex (especially in the prefrontal cortex), the CA1 subfield of the hippocampus, and the amygdala, as well as long-term potentiation deficits and altered basal synaptic transmission (Oddo et al., 2003b). At the behavioral level, these changes result in altered fear conditioning, impaired learning, and memory retention in the Morris water maze task (Billings et al., 2005) and poor performance in object recognition (Filali et al., 2012). By 20 months of age, extracellular Aβ plaques extend throughout the neocortex (especially in layers IV and V of the prefrontal cortex) and the CA1 area. At this advanced stage of the disease, neurofibrillary tangles are also evident in the hippocampus and the neocortex (Oddo et al., 2003b; Sy et al., 2011), alongside a considerable decrease in dendritic spine density (Bittner et al., 2010) and a significant reduction of the cerebral metabolism in cortical, subcortical, cerebellar, and brainstem regions (Nicholson et al., 2010).

* Corresponding author at: IDIBAPS, C/ Rosselló 149-153, 08036 Barcelona, Spain. Tel.: 34 932 275 400; fax: +34 932 271 890.
E-mail address: msanche3@clinic.ub.es (M.V. Sanchez-Vives).

https://doi.org/10.1016/j.neurobiolaging.2019.02.009

These neuropathological and behavioral AD-like hallmarks in the 3xTg-AD mouse model are likely to be accompanied by disturbances in cortical network activity. One way to assess these disturbances is by studying the spontaneously emergent activity of the cortical network, which integrates the neuronal intrinsic and synaptic properties and those of connectivity. Cortical slow oscillations (SO) occur during natural sleep and under anesthesia. They consist in a low-frequency ($\leq$1 Hz) rhythmic pattern in which cortical neurons fluctuate between active periods of neuronal firing and synaptic activity (Up states) and relatively inactive periods (Down states) (Steriade et al., 1993). Up states are generated by the cortical network itself, and are maintained by the network's recurrent excitatory and inhibitory synaptic connections. Furthermore, the activity pattern emerging during the Up states replicates and predicts some of the features during periods of cortical activation such as during rapid eye movement sleep and wakefulness (Destexhe et al., 2007; Steriade et al., 1996; Steriade and Timofeev, 2003).

SO rhythmic activity can provide relevant information about the network parameters that are compromised in the cerebral cortex of 3xTg-AD mice and also bring useful insights into the underlying alterations at the cellular and synaptic levels (Neske, 2016; Sanchez-Vives and Mattia, 2014). Impaired network synchronization has been reported in the hippocampus of 3xTg-AD mice (Akay et al., 2009; Squirrell, 2015), but cortical network disturbances have not been assessed in this strain. Thus, the aim of this study was to investigate whether 3xTg-AD mice presented any disturbances in cortical network activity at 2 different ages, to evaluate also changes associated with aging.

2. Methods

2.1. Animals

The 3xTg-AD mouse strain was genetically engineered at the University of California Irvine to express familial AD mutations of amyloid precursor protein (APPSwe), presenilin-1 (PS1M146V), and tau (tauP301L) (Oddo et al., 2003a,b). The mice included in this study were bred at the University of Barcelona and the Autonomous University of Barcelona and were provided by Drs Lydia Giménez-Llort and Coral Sanfeliu (Gimenez-Llort et al., 2007). To determine whether 3xTg-AD mice present disturbances in cortical network activity and to assess its evolution with aging, extracellular recordings were obtained from 7-month-old (3xTg $n = 18$; wild-type [Wt] $n = 14$) and 20-month-old (3xTg $n = 5$; Wt $n = 8$) adult mice of either sex. Mice were cared for and treated in accordance with Spanish regulatory laws (BOE-A-2013-6271), which comply with the European Union guidelines on protection of vertebrates used for experimentation (Directive 2010/63/EU of the European Parliament and the Council of 22 September 2010). All experiments were approved by the Ethics Committee at the Hospital Clinic de Barcelona (Spain). Mice were kept under standard conditions (room temperature at 23 $\pm$ 1 °C, 12:12-h light-dark cycle, lights on at 08:00 a.m.), with food (A04, Harlan, Spain) and water available *ad libitum* throughout the study.

2.2. In vivo extracellular recordings

Anesthesia was induced by means of intraperitoneal injection of ketamine (100 mg/kg) and medetomidine (1.3 mg/kg). Atropine (0.3 mg/kg) and methylprednisolone (30 mg/kg) were administered subcutaneously to prevent respiratory secretions and inflammation, respectively. A tracheotomy was performed to increase stability during the recordings. After this procedure, the mouse was placed in a stereotaxic frame and air enriched with oxygen was delivered to the mouse through a thin silicon tube placed at 0.5–1 cm from the tracheal cannula. Continuous infusion of ketamine (40 $mg \cdot kg^{-1} \cdot hour^{-1}$) was delivered subcutaneously with a pump to maintain a constant level of anesthesia (Castano-Prat et al., 2017; Ruiz-Mejias et al., 2011). Body temperature was maintained at 37 °C–38 °C throughout the experiment. Following Paxinos and Franklin (2008), bilateral craniotomies were made at 4 sites in each mouse: AP 2.3 mm from bregma, L 0.4 mm (prelimbic cortex [PrL] or medial prefrontal cortex); AP 0.5 mm, L 1.5 mm (primary motor cortex, M1); AP −1.5 mm, L 2.5 mm (primary somatosensory cortex, S1); and AP −2.5 mm, L 1.5 mm (primary visual cortex, V1). Recordings to survey local neuronal activity were obtained from deep layers (0.4 mm apart from the midline and 1.1–1.2 mm deep in PrL, 0.9–1.0 mm deep in M1, 0.8–0.9 mm deep in S1, and 0.8–0.9 mm deep in V1) by means of 1–2 MΩ tungsten microelectrodes (tip size less than 10 μm) insulated with a plastic coating except for the tip (FHC, Bowdoin, ME, USA). Spontaneous local field potential (LFP) recordings were obtained sequentially from each cortical area and simultaneously from left and right hemispheres. LFP recordings provide information about the local neuronal population—within 250 μm according to Katzner et al. (2009)—including synaptic potentials and, when high-pass-filtered, the multiunit activity (MUA). Multichannel LFP recordings of spontaneous activity from different areas therefore inform about the state of different neuronal ensembles, their firing rates, rhythmic activity, and synchronization at different frequency bands. All these parameters allow a detailed comparison between control and 3xTg-AD mice and an estimation of properties such as excitability and excitatory/inhibitory balance. In each animal, the 4 cortical areas were recorded in a counterbalanced order to avoid any influence of anesthesia levels, even though a constant level of anesthesia was maintained throughout the experiment. The signal was amplified with a multichannel system (Multi Channel Systems), digitized at 20 kHz with a CED acquisition board and acquired with Spike2 software (Cambridge Electronic Design) unfiltered.

2.3. Data analysis

To assess cortical network activity in 3xTg-AD and control mice, we analyzed and compared several parameters of the SO: its mean frequency, Up and Down state duration, the coefficient of variation (CV) of the Up-Down state cycle, and the population firing rate. Detection of Up and Down states from the recorded signals was based on 3 main fingerprints of the Up states: the slow LFP deflection, the gamma rhythm and the neuronal firing. These 3 features are reflected in 3 different time series: (1) the SO envelope; (2) the envelope of the variance of the gamma-filtered LFP (Mukovski et al., 2007); and (3) the estimation of MUA (Reig et al., 2010; Sanchez-Vives et al., 2010). From each LFP, we obtained a highly processed time series as a linear combination of these 3 features. The contribution of each one was weighted by principal component analysis by their projection into the first principal axis obtained in a principal component analysis. As the 3 signals correspond to 3 different frequency bands, this method is very robust against colored noise or band-limited electrode malfunction. Up and Down states were singled out by setting a threshold in this highly processed time series and the detection was done by an algorithm. This method has been widely used previously (e.g., Ruiz-Mejias et al., 2011, 2016; D'Andola et al., 2018). Parameters of the SO were computed from bilateral recordings in the 4 recorded areas. The frequency of the SO was the inverse of the duration of the whole Up-Down cycle. The CV of the SO frequency was the ratio between the standard deviation and the mean of the SO frequency.

The firing rate was based on the MUA signal. The MUA was estimated from the extracellular recordings as the power change in the Fourier components at frequencies between 200 and 1500 Hz in 5-ms windows (Reig et al., 2010; Sanchez-Vives et al., 2010). We

assumed that the spectrum within this frequency band provides a good estimate of the population firing rate because Fourier components at high frequencies have densities proportional to the spiking activity of the involved neurons (Mattia and Del Giudice, 2002). To obtain MUA time series (logMUA), MUA values were logarithmically scaled to balance the large fluctuations of the nearby spikes. The absolute values of firing rates during Up and Down states were computed as the mean of logMUA values during homologous periods. The relative firing rate was the maximum value of the logMUA averaged waveform after the Down-to-Up transition, after being normalized to zero during the Down states.

Finally, to analyze the fast components of the SO, we carried out Welch's power spectrum density analysis during Up and Down states, with 50% overlapped windows of 5000 samples. To highlight and compare peaks of neuronal synchronization over the intrinsic exponential decay of the signal, we computed the excess power, defined as the power ratio between power and the "*1/f*" decay.

2.4. Statistical analysis

Comparisons between right and left hemispheres were performed separately for each cortical area and parameter with the Student's *t*-test for dependent samples, corrected for multiple comparisons with the Bonferroni method (corrected $\alpha = 0.0125$). As we did not find any differences between right and left hemispheres, data from both hemispheres were averaged for each area and subject. Comparisons between groups and ages were performed by means of repeated measures two-way ANOVA for each parameter, setting the cortical area (PrL, M1, S1, and V1) as the within-subjects variable, and age (7 and 20 months of age) and group (Wt and 3xTg-AD) as between-subjects variables. Post hoc tests were performed with Student's *t*-tests for independent samples, corrected for multiple comparisons using the Bonferroni method (corrected $\alpha = 0.0125$). All the analyses were implemented in MATLAB (the MathWorks, Natick, MA, USA).

3. Results

Spontaneous rhythmic activity generated in the deep layers of different cortical regions (PrL, M1, S1, and V1; Fig. 1A) of 3xTg-AD and control mice was recorded under deep anesthesia at 7 and 20 months of age. Under these conditions, SO activity ($\leq$1 Hz) with alternating periods of intense synaptic activity and neuronal firing (Up states) and rather quiescent periods (Down states) was generated in the thalamocortical network (Fig. 1B, top) (Steriade et al., 1993). Fast rhythms (beta-gamma, 15–100 Hz) were also detected (Fig. 1B, bottom), mainly confined to the Up states (Compte et al., 2008; Steriade et al., 1996). Following previous studies (Castano-Prat et al., 2017; Ruiz-Mejias et al., 2011;

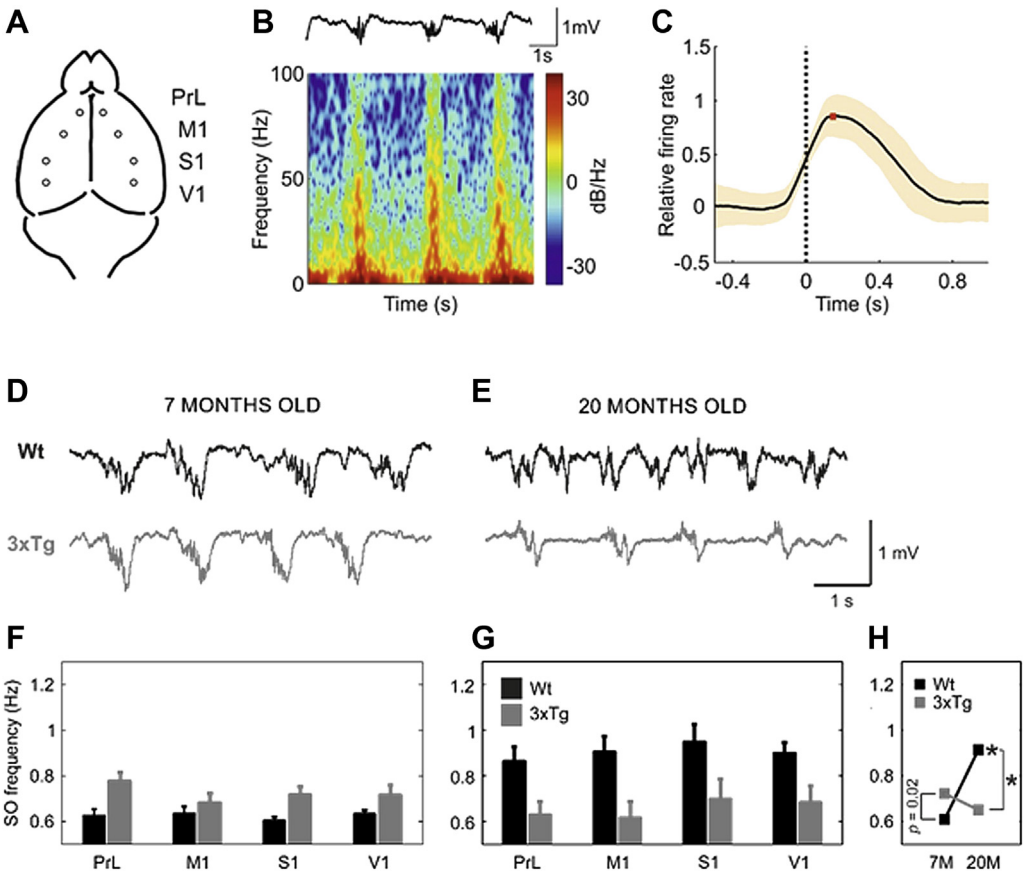

Fig. 1. Spontaneous oscillatory activity in the 3xTg-AD mouse. (A): Extracellular activity in deep layers was recorded simultaneously in both hemispheres in each cortical area. (B): Top: Raw local field potential (LFP) from the right PrL cortex of a wild-type (Wt) mouse showing slow oscillations (SO) with alternating Up (active) and Down (silent) states. Bottom: Spectrogram corresponding to the LFP showing high-frequency rhythms, mainly during the Up states. (C): Waveform average of the mean multiunit activity (MUA) signal aligned at the Down-to-Up state transition (dashed line at time 0). This average was used to calculate the maximum firing rate (red square; see *Materials and Methods* for details). Shade represents the SD. (D–E): Raw LFP recordings from right M1 at 7 and 20 months, respectively, in Wt (black) and 3xTg-AD (gray) mice. (F–G): Population data comparing the SO frequency between 3xTg-AD and Wt mice at 7 and 20 months of age, respectively, in the 4 cortical areas. (H): Population data showing the evolution of SO frequency between 7 and 20 months in both groups, with the 4 cortical areas pooled together. Bars and squares depict the mean, error bars are SE. * $p < 0.0125$ 3xTg versus Wt mice and 7 versus 20 months of age in (H). Abbreviations: AD, Alzheimer's disease; PrL, prelimbic cortex; M, months old; M1, primary motor cortex; S1, primary somatosensory cortex; V1, primary visual cortex. (For interpretation of the references to color in this figure legend, the reader is referred to the Web version of this article.)

Table 1
Results of the repeated measures two-way ANOVA for each analyzed parameter in the 3xTg-AD mouse model

Parameter	Intrasubject factor: Cortical area			Intersubject factor: group			Intersubject factor: Age			Interactions			
	F	*p*	Effect size (η^2)	*F*	*p*	Effect size (η^2)	*F*	*p*	Effect size (η^2)	Type	*F*	*p*	Effect size (η^2)
SO freq.	0.82	0.48	0.02	3.44	0.07	0.077	6.9	**0.01**	0.144	group × age	18.6	**<0.0001**	0.313
Up dur.	10.41	**<0.0001**	0.203	1.11	0.29	0.026	10.38	**0.002**	0.202	area × age	3.28	**0.02**	0.074
										group × age	24.64	**<0.0001**	0.375
Down dur.	0.54	0.65	0.013	11.87	**0.001**	0.225	0.68	0.41	0.016	area × group	3.3	**0.02**	0.075
										group × age	19.2	**<0.0001**	0.320
SO CV	2.82	**0.04**	0.064	9.01	**0.005**	0.180	2.63	0.11	0.06	group × age	10.28	**0.003**	0.201
FR Up	54.092	**<0.0001**	0.569	0.001	0.976	<0.0001	383.084	**<0.0001**	0.903	area × age	3.146	**0.028**	0.071
										area × group	6.049	**0.001**	0.129
										group × age	5.715	**0.021**	0.122
FR Down	29.533	**<0.0001**	0.425	2.585	0.116	0.061	350.961	**<0.0001**	0.898	area × group	5.077	**0.002**	0.113
FR rel.	49.981	**<0.0001**	0.549	6.696	**0.013**	0.140	34.921	**<0.0001**	0.460	area × age	3.563	**0.016**	0.080
										area × group	3.013	**0.033**	0.068
										group × age	13.072	**0.001**	0.242

Comparisons between groups and ages were performed with cortical area (PrL, prelimbic; M1, primary motor; S1, primary somatosensory; V1, primary visual) as the within-subjects variable, and age (7 and 20 mo of age) and group (control—wild type—and 3xTg-AD) as between-subjects variables. Post hoc tests were performed with Student's *t*-test for independent samples, corrected for multiple comparisons using the Bonferroni method (corrected $\alpha = 0.0125$).
Bold text indicates $p < 0.05$.
Key: SO, slow oscillation; freq, frequency; CV, coefficient of variation; FR, firing rate; rel, relative; dur, duration.

Sanchez-Vives et al., 2010), several parameters of the oscillatory activity were quantified and compared between 3xTg-AD and control mice: frequency of the SO, Up state duration, Down state duration, the coefficient of variation of the Up-Down state cycle, the population firing rate (Fig. 1C) and the high-frequency content during the Up states. LFP recordings were obtained bilaterally, but no differences were found between hemispheres, neither for any of the analyzed parameters and cortical areas nor in any of the 2 groups; therefore, data of both hemispheres were averaged for each cortical area and animal.

3.1. SO frequency and its variability are altered in the anesthetized 3xTg-AD mouse model

The mean SO frequency differed between 3xTg and control groups at 20 months, but not at 7 months. (group × age interaction, Table 1, Fig. 1D–H). At 7 months, the frequency of the SO tended to be higher in 3xTg mice (Fig. 1D, F and H), although this did not reach the significance threshold established in the study. At 20 months of age, however, the frequency of the SO was significantly lower in 3xTg than in control mice (Fig. 1E, G, H). The reversal of the trend at 20 months of age was due to the SO frequency being differently modulated by age in each group, increasing in control animals between 7 and 20 months of age, but remaining rather stable—with a tendency to decrease—in 3xTg animals (Fig. 2H).

The tendency of 7-month-old 3xTg mice to have a higher SO frequency can be explained by the shorter Up states (Fig. 2D, F) because at this age, Down state duration did not differ between the 2 groups (Fig. 2A, C). Between 7 and 20 months of age, Down and Up state duration changed differentially in the 2 groups: Down state duration decreased in control animals but increased in the 3xTg ones (group × age interaction, Table 1; Fig. 2C), and a similar pattern was observed for the Up state duration, which decreased in control animals, but remained rather stable—with a slight tendency

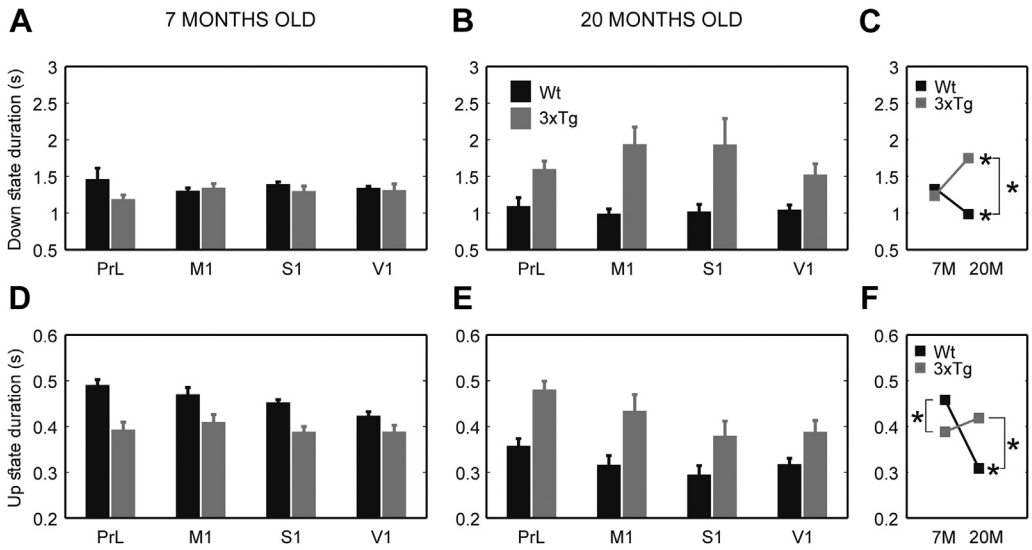

Fig. 2. Up and Down state duration in the 3xTg-AD mouse. (A,B): Population data comparing Down state duration between 3xTg-AD and control mice at 7 and 20 months of age, respectively, in the 4 cortical areas. (D,E): Same as aforementioned, comparing Up state duration. (C,F): Population data showing the evolution of Down and Up state duration, respectively, between 7 and 20 months in both groups, with the 4 cortical areas pooled together. Bars and symbols depict the mean, error bars are SE. * $p < 0.0125$ 3xTg versus control mice and 7 versus 20 months of age in (C and F). Abbreviations: AD, Alzheimer's disease; PrL, prelimbic cortex; M, months old; M1, primary motor cortex; S1, primary somatosensory cortex; V1, primary visual cortex; Wt, wild type.

to increase—in the 3xTg ones (group × age interaction, Table 1; Fig. 2F). As a result of this differential evolution, at 20 months of age, Down and Up state durations were significantly longer in 3xTg mice (Fig. 2B,C and E, F, respectively) whose SO frequency was consequently reduced (Fig. 1G, H).

Besides showing a lower SO frequency, the SO cycle was more irregular in 20-month-old 3xTg mice than in their age-matched controls (Fig. 3). This irregularity can be appreciated in raster plots illustrating consecutive Up states aligned at their Down-to-Up transition (Fig. 3A, B), which substantiate the elongation of Up and Down states in 20-month-old 3xTg mice and demonstrate a higher temporal irregularity in this group. We corroborated these observations at the population level: at 7 months of age, the mean CV of the SO did not differ between groups (Fig. 3C, E), but toward 20 months of age, the CV of the SO evolved differently (group × age interaction, Table 1; Fig. 3E), augmenting in the 3xTg animals but remaining stable in the controls (Fig. 3E), leading to a higher CV of the SO at 20 months of age in the 3xTg animals (Fig. 3D, E).

3.2. Relative firing rate is reduced in the anesthetized 3xTg-AD mouse model at advanced ages

The population firing rate during Up and Down states was calculated as the power change in the Fourier components between 200 and 1500 Hz (Castano-Prat et al., 2017; Reig et al., 2010; Ruiz-Mejias et al., 2011), which is a good estimation of spiking activity of the neurons surrounding the electrode tip (Mattia and Del Giudice, 2002). We also computed a relative measure of the firing rate—the relative firing rate—representing the population spiking activity during Up states with respect to the spiking activity during the Down states (Fig. 1C; see *Materials and Methods* for further details).

While it is true Down states are considered relatively silent states with respect to Up states, there is some firing in Down states (Shu et al., 2003), and it has been proposed that this is critical for the initiation of Up states (Compte et al., 2003). The firing rate during Down states is modulated by physiological conditions such as temperature (Reig et al. (2010) and that there is a relationship between the firing rate in Down states and the frequency of the SO (D'Andola et al., 2018).

Firing rate increased with age in both groups (Fig. 4). While the mean firing rate during Down and Up states was comparable between groups at 7 months of age (no main effect of group, Table 1; Fig. 4A, D), it had increased significantly by 20 months (main effect of age, Table 1; Fig. 4B, C), the mean firing rate during Up states bearing a greater increase in controls (group × age interaction, Table 1; Fig. 4E, F). As a consequence, between 7 and 20 months of age, the relative firing rate increased more markedly in control animals, resulting in a significantly lower relative firing rate in 20-month-old 3xTg animals than in their age-matched controls, whereas at 7 months, such difference was not observed (group × age interaction, Table 1; Fig. 4G–I).

In both groups, the magnitude of the firing rate during the Down states was inversely related to its duration: longer Down states had lower firing rates, in agreement with previous findings (Compte et al., 2003; Sanchez-Vives et al., 2017) (Fig. 4J, K). However, although the increase in firing rate during the Down states occurring between 7 and 20 months of age (Fig. 4C) happened in parallel to the shortening of Down states in control animals (see Fig. 3C), this was not the case in the 3xTg animals, who showed an elongation of the Down states (see Fig. 3C). This suggests that the firing rate occurring during the Down states was less efficient in generating Up states in the 3xTg mice at 20 months (Fig. 4A and Fig. 2A, respectively). In addition, the firing rate during Down states and the SO frequency were related: higher firing rate during Down states was associated with higher SO frequency (Fig. 4L, M). However, at 20 months, there was a decrease in the correlation between the firing rate during the Down states and Down state duration in the 3xTg animals from 7 to 20 months (Fig. 4J vs. Fig. 4K) along with a decline in the correlation between SO frequency and firing rate during the Down states in this group (Fig. 4L vs. Fig. 4M), illustrating a disruption in the dynamical balance of the network.

3.3. Abnormal synchronization of beta and gamma frequencies during the Up states in the anesthetized 3xTg-AD mouse model

Finally, we studied the high-frequency content (beta and gamma oscillations, 15–100 Hz) during Up and Down states in 3xTg and control mice because synchronization in this band has been linked

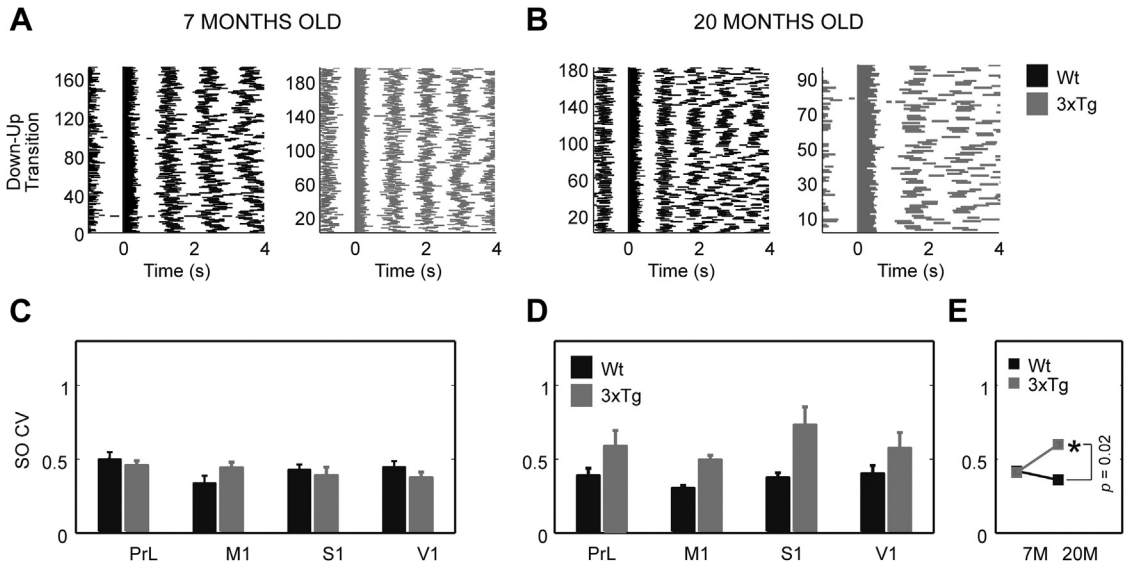

Fig. 3. Coefficient of variation (CV) of the SO in the 3xTg-AD mouse. (A,B): Representative raster plots showing aligned Up states (detected during 200 seconds) in M1 at 7 and 20 months of age, respectively, in one control (black) and one 3xTg (gray) mouse. (C,D): Population data comparing the CV of the SO between 3xTg-AD and control mice at 7 and 20 months of age, respectively, in the 4 cortical areas. (E): Population data showing the evolution of the CV of the SO between 7 and 20 months of age in both groups, with the 4 cortical areas pooled together. Bars and squares depict the mean, error bars are SE. * $p < 0.0125$ 3xTg versus control mice and 7 versus 20 months of age in (E). Abbreviations: SO, slow oscillations; AD, Alzheimer's disease; PrL, prelimbic cortex; M, months old; M1, primary motor cortex; S1, primary somatosensory cortex; V1, primary visual cortex; Wt, wild type.

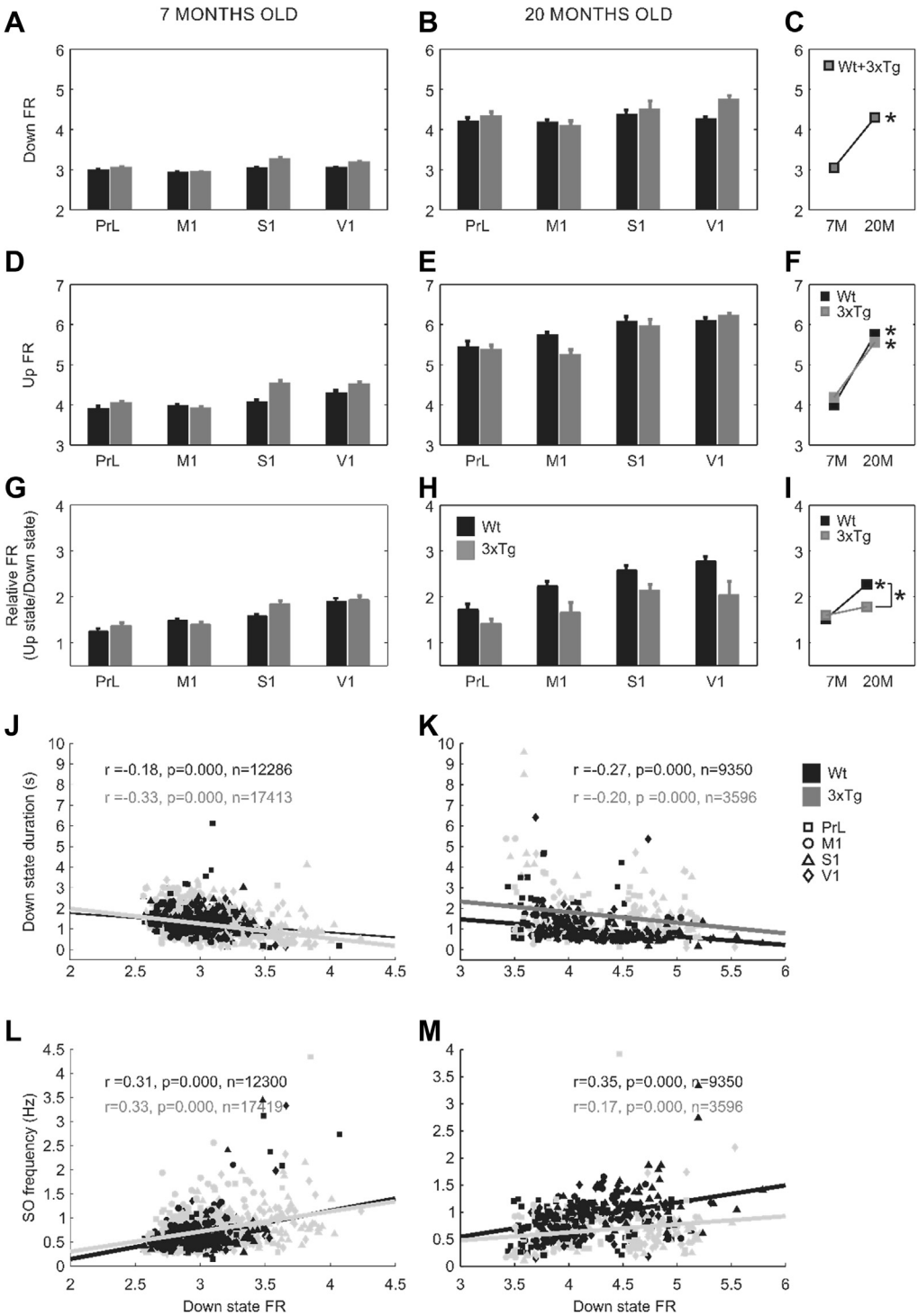

Fig. 4. Population firing rate in the 3xTg-AD mouse. (A, B): Population data comparing firing rate (FR) during Down states between control (black) and 3xTg-AD mice (gray) at 7 and 20 months of age, respectively, in the 4 cortical areas. (D, E): Same as aforementioned, comparing FR during Up states. (G, H): Same as aforementioned, comparing the relative (Up/Down) FR. (C): Population data showing the evolution of the FR during the Down states between 7 and 20 months of age, with both groups and the 4 cortical areas pooled together. (F, I): Population data showing the evolution of the FR during Up states and the relative FR, respectively, between 7 months and 20 months of age in both groups, with the 4 cortical areas pooled together. (J, K): Pearson's correlation between the FR during Down states and the Down state duration at 7 and 20 months of age, respectively, in the 4 cortical areas. (L, M): Same as aforementioned, between the FR during Down states and the frequency of the SO. Bars and squares depict the mean, error bars are SE. * $p < 0.0125$ 3xTg versus control mice and 7 versus 20 months of age in (C, F, I). Abbreviations: SO, slow oscillations; AD, Alzheimer's disease; FR, firing rate; PrL, prelimbic cortex; M, months old; M1, primary motor cortex; S1, primary somatosensory cortex; V1, primary visual cortex; Wt, wild type; 7M, 7 months old; 20M, 20 months old.

to cognitive and perceptual processes (Siegel et al., 2012; Wang, 2010). We found that the mean power spectrum of 3xTg mice significantly differed from that of controls at both ages, with heterogeneity depending on the cortical area.

In both groups, PrL and M1 cortical areas presented a modulation centered at 40–50 Hz during the Up states (Fig. 5A–D), although in 20-month-old 3xTg animals, the synchronization of the activity cortex did not form a peak in the power spectrum as clearly

as in controls (especially in M1) (Fig. 5B, D). In S1 and V1 (Fig. 5E–H), the synchronization peaks during the Up states were only clearly observed when calculating the excess power (see *Materials and Methods*), revealing that these peaks occurred at lower frequencies than those in the PrL and M1 cortices, at both ages (Fig. 5E–H, vertical lines in the insets). Thus, anterior cortical areas (PrL, M1) synchronized their activity during the Up states at higher frequencies (ca. 50 Hz) than posterior areas (S1, V1) (ca. 30–40 Hz), and this tendency was preserved in the 3xTg group.

As control animals got older, the amplitude of the synchronization peak during the Up states was reduced in all cortical areas except for the S1 area, where its amplitude increased (Fig. 5B, D, F, and H, black arrowheads vs. black solid lines in the insets). We also observed the decrease in the amplitude of the synchronization peak with increasing age in the PrL and M1 cortices of 3xTg animals (Fig. 5B, D, magenta arrowheads vs. red solid lines in the insets), but we detected group differences in S1 and V1: the large amplitude of the S1 area synchronization peak observed in 20-month-old control

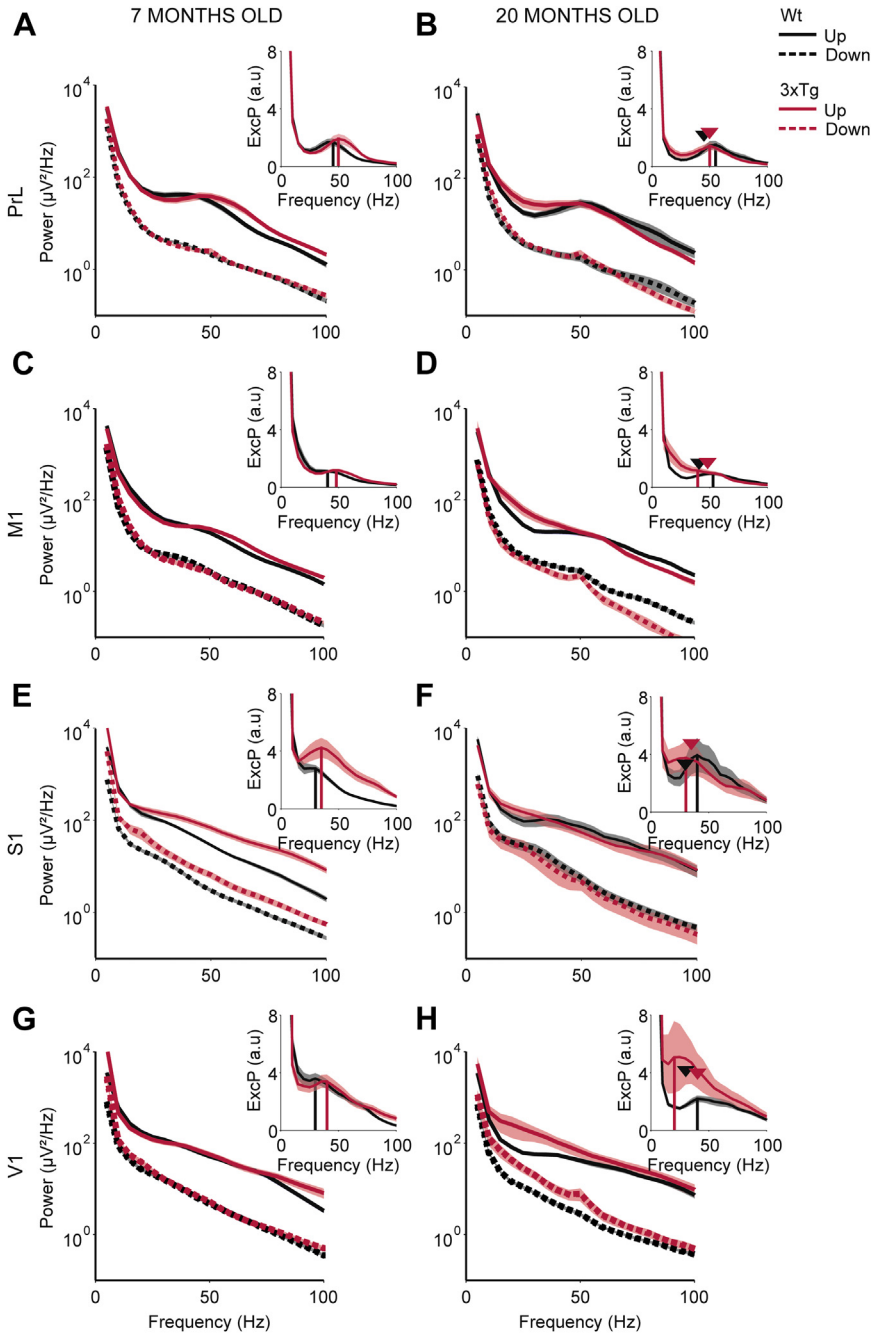

Fig. 5. High frequency content of the SO in the 3xTg-AD mouse. (A–H): Mean raw power spectra of control (black) and 3xTg-AD (magenta) mice at 7 (left) and 20 (right) months of age in PrL (A, B), M1 (C, D), S1 (E, F), and V1 (G, H) cortices, during Up (solid lines) and Down states (dashed lines). Insets show excess power (ExcP) during the Up states, defined as the ratio between the mean power during Up states and the fit of the "*1/f*" decay of the power spectrum. Vertical lines in the insets indicate the power peak for each group. Arrowheads in the insets in (B, D, F, and H) indicate the frequency and amplitude of the power peak at 7 months. Shade is the SE. a.u. (arbitrary units). Abbreviations: SO, slow oscillations; AD, Alzheimer's disease; PrL, prelimbic cortex; M1, primary motor cortex; S1, primary somatosensory cortex; V1, primary visual cortex; Wt, wild type. (For interpretation of the references to color in this figure legend, the reader is referred to the Web version of this article.)

animals was already present in 7-month-old 3xTg mice (Fig. 5E, F), suggesting it to be a sign of earlier aging; furthermore, V1 area synchronization peak also increased with age in 3xTg animals (Fig. 5H, arrowheads vs. solid lines in the insets).

The mean power spectrum differences between control and 3xTg animals during the Down states were not as pronounced and consistent across cortical areas (Fig. 5A–H, dashed lines) as during the Up states. At 7 months of age, the mean power spectrum during Up states appeared to be displaced toward higher frequencies in 3xTg animals with respect to controls (Fig. 5A, C, E, G, solid lines); this displacement was especially pronounced in the PrL and M1 cortices, but was apparent in all the cortical areas as a shift toward higher frequencies in the synchronization peak of the excess power (Fig. 5A, C, E, G, vertical lines in the insets). However, at 20 months of age, the pattern was reversed, and the mean power spectrum of 3xTg animals was then located at lower frequencies than that of controls (Fig. 5B, D, F, H, solid lines). This inversion was due to the fact that high frequency content during Up states evolved differently in both groups as they got older: from 7 to 20 months, the synchronization peak of high frequencies during the Up states moved toward higher frequencies in control animals, but toward lower frequencies in 3xTg animals (Fig. 5B, D, F, H, arrowheads vs. solid lines in the insets).

4. Discussion

We compared the Up and Down states of the spontaneously generated cortical SO, alongside the fast (beta and gamma) rhythms during Up states between the 3xTg-AD mouse model of AD and control mice at 7 and 20 months of age. 3xTg-AD mice presented alterations in the emergent cortical activity with respect to controls, and the electrophysiological phenotype of 3xTg-AD animals changed with age in a different manner compared to that of control animals. Almost all changes between 3xTg and control mice were detected at 20 months of age: 3xTg mice presented lower SO frequency (consistent with longer Up and Down states), higher Up-Down cycle variability, lower relative firing rate, and a shift of the high-frequency rhythms toward lower frequencies, similarly to one of the electroencephalography hallmarks of AD in humans (Jeong, 2004). The only change detected at 7 months of age was the reduction of Up state duration in 3xTg animals with respect to controls. The absence of more alterations in the cortical network physiology at that age is surprising, considering that 7-month-old 3xTg animals present with intracellular Aβ immunoreactivity in the neocortex (Oddo et al., 2003b) and behavioral deficits (Billings et al., 2005; Filali et al., 2012). We would suggest that larger alterations are needed to affect a pattern as robust and conserved as the SO (Sanchez-Vives et al., 2017). These major alterations are indeed present in 20-month-old 3xTg animals, in which Aβ plaques and neurofibrillary tangles are detectable throughout the neocortex (Oddo et al., 2003b; Sy et al., 2011), a considerable decrease in dendritic spines density has occurred (Bittner et al., 2010), and the cerebral metabolism in cortical regions is already significantly reduced (Nicholson et al., 2010). Altogether, this suggests that these alterations are responsible for SO alterations detected in the present work at 20 months, and that the intracellular Aβ accumulation is not enough to cause significant changes in the SO parameters characterized here.

The increase in the slow oscillation frequency that occurred between 7 and 20 months of age in control animals did not take place in the 3xTg animals. In the 3xTg-AD mouse, the Up state duration remained stable throughout the 2 studied ages, whereas the Down state duration significantly increased between 7 and 20 months of age. The transition from the Up state to the Down state has been proposed to be mediated by inhibitory interneurons (Funk et al., 2017; Zucca et al., 2017) and/or by the accumulation of activity-dependent potassium conductances (Compte et al., 2003; Roopun et al., 2006; Sanchez-Vives and McCormick, 2000), mechanisms that are activity-dependent (Sanchez-Vives et al., 2010). The firing rates during Down and Up states increased in control and 3xTg animals as they got older, along with the expected shorter Up states in control animals, but not in 3xTg animals. This suggests that during the aging process, the physiological dynamic relationships regulating the oscillatory pattern were altered in the 3xTg-AD mouse. Alterations in the oscillatory dynamics during slow wave sleep could be associated with sleep alterations in AD, associated per se with cognitive decline (Ju et al., 2014).

An increase in cortical excitability associated with aging was also reflected in the firing rate during the Down states, which increased from 7 to 20 months of age in both groups of animals. This is coherent with the shortening of Down states that was observed in control animals as they got older, as high-frequency fluctuations during the Down state facilitate the generation of the subsequent Up state (Compte et al., 2003; Sanchez-Vives et al., 2017). However, in the 3xTg-AD mouse model, the increase in firing rate during the Down states that occurs between 7 and 20 months of age was accompanied by an elongation of the Down states, revealing an increased threshold for recruiting the local network and trigger Up states.

Thus, the evolution of SO parameters as 3xTg-AD animals get older reveals difficulties to transition between states and thus in a loss of flexibility of the cortical network. This could be the result of the cellular and synaptic alterations presented by 3xTg-AD animals at 20 months of age, such as the presence of extracellular Aβ deposits (Oddo et al., 2003a; Sy et al., 2011) or the loss of dendritic spines (Bittner et al., 2010), and may be contributing to the cognitive deficits reported in these animals, as higher cognitive functions require a flexible modulation of the interactions between the neuronal groups belonging to a given cortical network (Bressler and Kelso, 2001; Fries, 2005).

Because the periodicity of the oscillatory cycle depends on the interaction between the mechanisms involved in Up state initiation and termination (reviewed by Neske, 2016), the SO variability in 20-month-old 3xTg animals was increased. The loss of cholinergic receptors in 3xTg-AD mice (Billings et al., 2005), also reported in humans with AD (Coyle et al., 1983), may contribute as the rhythmicity of the SO diminishes when cortical cholinergic tone is reduced (Lorincz et al., 2015).

The synchronization peak of high (beta-gamma) frequencies during the Up state was detected at higher frequencies in 3xTg than in control animals at 7 months old, but at lower frequencies at 20 months. The dominant frequency of beta-gamma oscillations depends critically on the magnitude and temporal course of the inhibitory feedback (Compte et al., 2008; Cunningham et al., 2004). The displacement of the high-frequency synchronization peak that both groups presented as they got older suggests that although the cortical network of 3xTg animals might be more excitable than that of the control group at 7 months of age, at 20 months of age, this network is more inhibited, and that while the excitability of the cortical network increases in the control animals with age, it decreases in the case of the 3xTg animals. Reduced cortical excitability in the 20-month-old 3xTg animals is consistent with the lower relative firing rate and with the longer Up states due to decreased activity-dependent potassium conductances (Sanchez-Vives et al., 2010). In fact, lower high frequencies are commonly described EEG spectral alterations in patients with AD (Dierks et al., 2000; Huang et al., 2000; Lizio et al., 2011) and have been related to the deterioration of global cognitive function (Jeong, 2004; Kowalski et al., 2001; Sloan et al., 1995). The shift toward lower frequencies of the beta-gamma synchronization peak in the 20-

month-old 3xTg animals is reminiscent of this alteration and indicates that their electrophysiological phenotype is consistent with that of humans with AD and other mouse models of the disease (Castano-Prat et al., 2017). This suggests that the alteration of the inhibitory component of the network described in advanced AD stages in humans (Francis et al., 1999) could be relevant to the pathophysiology of the disease.

It has been reported that ketamine anesthesia enhances gamma power (Hong et al., 2009; Hunt et al., 2010; Lazarewicz et al., 2009). This could be a confounding factor in the reported results; however, both Wt and 3xTg-AD animals were recorded under the same anesthesia, and therefore, we should attribute the observed differences to changes in the network. Still, we should mention that a potential interaction between the anesthesia and the disease could eventually occur, although we did not observe differences in the required anesthesia doses. This is one of the problems that are encountered when comparing brain activity in Wt versus diseased animals: not only diseased animals could respond differently to the anesthesia, but if studying wakefulness, there could be also a different alert state. In previous studies in Dyrk1A (Down Syndrome model) in which a decreased gamma generation was observed during Up states, the same was the case when awake mice were recorded (Ruiz-Mejias et al., 2016). Still, further studies with chronically implanted animals will be useful in the case of AD to establish whether the alterations that we describe in high frequencies remain in the awake state.

In conclusion, SO parameters evolved in a different manner in control and 3xTg-AD animals although they were quite similar at 7 months of age. In particular, 20-month-old 3xTg animals presented with lower SO frequency, longer Up and Down states, higher SO variability, lower relative firing rate, and a shift toward lower frequencies of the mean power spectrum during the Up states with respect to age-matched Wt controls, the latter of which mimics one of the features in humans with AD, corroborating the suitability of the 3xTg mouse as a model for this disorder. The evolution of the SO parameters as 3xTg animals get older also points to an alteration of the network mechanisms involved in the transitions between Up and Down states, resulting in a less flexible cortical network that struggles to transition between states. Decreased excitability and flexibility of the cortical network in older 3xTg-AD animals is the result of cellular and synaptic alterations and may be contributing to the cognitive deficits reported in this model.

Our results help to unveil the cortical network functional alterations in AD, which probably underlie also cognitive deficits commonly observed in AD, and may have practical implications in preclinical research, such as allowing the tracking of the impact of novel molecules aimed at modifying the course of neuronal dysfunctions in this AD model. In other pathologies such as Fragile X syndrome (Castano-Prat et al., under review), we have observed how genetic and pharmacological interventions reverse slow wave alterations along with other manifestations of the disease. Because we have found that SO alterations increase with age, along with other structural and functional changes described in other works, specific changes in cortical oscillatory networks may be helpful to predict to what extent cognitive dysfunctions are likely to evolve with the disease.

Disclosure

The authors declare no conflict of interest.

Acknowledgements

The authors thank Dr. C. Gonzalez-Liencres for editing assistance.

This work was supported by Ministerio de Economía y Competividad (Spain, BFU2017-85048-R), FLAG-ERA (PCIN-2015-162-C02-01), and CERCA Programme/Generalitat de Catalunya.

Appendix A. Supplementary data

Supplementary data associated with this article can be found, in the online version, at https://doi.org/10.1016/j.neurobiolaging.2019.02.009.

References

Akay, M., Wang, K., Akay, Y.M., Dragomir, A., Wu, J., 2009. Nonlinear dynamical analysis of carbachol induced hippocampal oscillations in mice. Acta Pharmacol. Sin. 30, 859–867.

Billings, L.M., Oddo, S., Green, K.N., McGaugh, J.L., LaFerla, F.M., 2005. Intraneuronal Abeta causes the onset of early Alzheimer's disease-related cognitive deficits in transgenic mice. Neuron 45, 675–688.

Bittner, T., Fuhrmann, M., Burgold, S., Ochs, S.M., Hoffmann, N., Mitteregger, G., Kretzschmar, H., LaFerla, F.M., Herms, J., 2010. Multiple events lead to dendritic spine loss in triple transgenic Alzheimer's disease mice. PLoS One 5, e15477.

Bressler, S.L., Kelso, J.A.S., 2001. Cortical coordination dynamics and cognition. Trends Cogn. Sci. 5, 26–36.

Castano-Prat, P., Perez-Zabalza, M., Perez-Mendez, L., Escorihuela, R.M., Sanchez-Vives, M.V., 2017. Slow and fast neocortical oscillations in the senescence-accelerated mouse model SAMP8. Front. Aging Neurosci. 9, 141.

Compte, A., Sanchez-Vives, M.V., McCormick, D.A., Wang, X.J., 2003. Cellular and network mechanisms of slow oscillatory activity (<1 Hz) and wave propagations in a cortical network model. J. Neurophysiol. 89, 2707–2725.

Compte, A., Reig, R., Descalzo, V.F., Harvey, M.A., Puccini, G.D., Sanchez-Vives, M.V., 2008. Spontaneous high-frequency (10-80 Hz) oscillations during up states in the cerebral cortex in vitro. J. Neurosci. 28, 13828–13844.

Coyle, J.T., Price, D.L., DeLong, M.R., 1983. Alzheimer's disease: a disorder of cortical cholinergic innervation. Science 219, 1184–1190.

Cunningham, M.O., Whittington, M.A., Bibbig, A., Roopun, A., LeBeau, F.E.N., Vogt, A., Monyer, H., Buhl, E.H., Traub, R.D., 2004. A role for fast rhythmic bursting neurons in cortical gamma oscillations in vitro. Proc. Natl. Acad. Sci. U. S. A. 101, 7152–7157.

Destexhe, A., Hughes, S.W., Rudolph, M., Crunelli, V., 2007. Are corticothalamic "up" states fragments of wakefulness? Trends Neurosci. 30, 334–342.

Dierks, T., Jelic, V., Pascual-Marqui, R.D., Wahlund, L., Julin, P., Linden, D.E., Maurer, K., Winblad, B., Nordberg, A., 2000. Spatial pattern of cerebral glucose metabolism (PET) correlates with localization of intracerebral EEG-generators in Alzheimer's disease. Clin. Neurophysiol. 111, 1817–1824.

D'Andola, M., Weinert, J.F., Mattia, M., Sanchez-Vives, M.V., 2018. Modulation of slow and fast oscillations by direct current stimulation in the cerebral cortex in vitro. bioRxiv 246819.

Filali, M., Lalonde, R., Theriault, P., Julien, C., Calon, F., Planel, E., 2012. Cognitive and non-cognitive behaviors in the triple transgenic mouse model of Alzheimer's disease expressing mutated APP, PS1, and Mapt (3xTg-AD). Behav. Brain Res. 234, 334–342.

Francis, P.T., Palmer, A.M., Snape, M., Wilcock, G.K., 1999. The cholinergic hypothesis of Alzheimer's disease: a review of progress. J. Neurol. Neurosurg. Psychiatry 66, 137–147.

Fries, P., 2005. A mechanism for cognitive dynamics: neuronal communication through neuronal coherence. Trends Cogn. Sci. 9, 474–480.

Funk, C.M., Peelman, K., Bellesi, M., Marshall, W., Cirelli, C., Tononi, G., 2017. Role of somatostatin-positive cortical interneurons in the generation of sleep slow waves. J. Neurosci. 37, 9132–9148.

Gimenez-Llort, L., Blazquez, G., Canete, T., Johansson, B., Oddo, S., Tobena, A., LaFerla, F.M., Fernandez-Teruel, A., 2007. Modeling behavioral and neuronal symptoms of Alzheimer's disease in mice: a role for intraneuronal amyloid. Neurosci. Biobehav. Rev. 31, 125–147.

Hong, L.E., Summerfelt, A., Buchanan, R.W., O'Donnell, P., Thaker, G.K., Weiler, M.A., Lahti, A.C., 2009. Gamma and delta neural oscillations and association with clinical symptoms under subanesthetic ketamine [online]. Neuropsychopharmacology 35, 632.

Huang, C., Wahlund, L., Dierks, T., Julin, P., Winblad, B., Jelic, V., 2000. Discrimination of Alzheimer's disease and mild cognitive impairment by equivalent EEG sources: a cross-sectional and longitudinal study. Clin. Neurophysiol. 111, 1961–1967.

Hunt, M.J., Falinska, M., Łęski, S., Wójcik, D.K., Kasicki, S., 2010. Differential effects produced by ketamine on oscillatory activity recorded in the rat hippocampus, dorsal striatum and nucleus accumbens. J. Psychopharmacol. 25, 808–821.

Jeong, J., 2004. EEG dynamics in patients with Alzheimer's disease. Clin. Neurophysiol. 115, 1490–1505.

Ju, Y.-E.S., Lucey, B.P., Holtzman, D.M., 2014. Sleep and Alzheimer disease pathology–a bidirectional relationship. Nat. Rev. Neurol. 10, 115–119.

Katzner, S., Nauhaus, I., Benucci, A., Bonin, V., Ringach, D.L., Carandini, M., 2009. Local origin of field potentials in visual cortex. Neuron 61, 35–41.

Kowalski, J.W., Gawel, M., Pfeffer, A., Barcikowska, M., 2001. The diagnostic value of EEG in Alzheimer disease: correlation with the severity of mental impairment. J. Clin. Neurophysiol. 18, 570–575.
LaFerla, F.M., Oddo, S., 2005. Alzheimer's disease: abeta, tau and synaptic dysfunction. Trends Mol. Med. 11, 170–176.
Lazarewicz, M.T., Ehrlichman, R.S., Maxwell, C.R., Gandal, M.J., Finkel, L.H., Siegel, S.J., 2009. Ketamine modulates theta and gamma oscillations. J. Cogn. Neurosci. 22, 1452–1464.
Lizio, R., Vecchio, F., Frisoni, G.B., Ferri, R., Rodriguez, G., Babiloni, C., 2011. Electroencephalographic rhythms in Alzheimer's disease. Int. J. Alzheimers Dis. 2011, 927573.
Lorincz, M.L., Gunner, D., Bao, Y., Connelly, W.M., Isaac, J.T.R., Hughes, S.W., Crunelli, V., 2015. A distinct class of slow (~0.2-2 Hz) intrinsically bursting layer 5 pyramidal neurons determines UP/DOWN state dynamics in the neocortex. J. Neurosci. 35, 5442–5458.
Mattia, M., Del Giudice, P., 2002. Population dynamics of interacting spiking neurons. Phys. Rev. E. Stat. Nonlin. Soft Matter Phys. 66, 51917.
Mukovski, M., Chauvette, S., Timofeev, I., Volgushev, M., 2007. Detection of active and silent states in neocortical neurons from the field potential signal during slow-wave sleep. Cereb. Cortex 17, 400–414.
Neske, G.T., 2016. The slow oscillation in cortical and thalamic networks: mechanisms and functions. Front. Neural Circuits 9, 88.
Nicholson, R.M., Kusne, Y., Nowak, L.A., LaFerla, F.M., Reiman, E.M., Valla, J., 2010. Regional cerebral glucose uptake in the 3xTG model of Alzheimer's disease highlights common regional vulnerability across AD mouse models. Brain Res. 1347, 179–185.
Oddo, S., Caccamo, A., Kitazawa, M., Tseng, B.P., LaFerla, F.M., 2003a. Amyloid deposition precedes tangle formation in a triple transgenic model of Alzheimer's disease. Neurobiol. Aging 24, 1063–1070.
Oddo, S., Caccamo, A., Shepherd, J.D., Murphy, M.P., Golde, T.E., Kayed, R., Metherate, R., Mattson, M.P., Akbari, Y., LaFerla, F.M., 2003b. Triple-transgenic model of Alzheimer's disease with plaques and tangles: intracellular Abeta and synaptic dysfunction. Neuron 39, 409–421.
Paxinos, G., Franklin, K., 2008. The Mouse Brain in Stereotaxic Coordinates, third ed. Academic Press, Cambridge, MA.
Querfurth, H.W., LaFerla, F.M., 2010. Alzheimer's disease. N. Engl. J. Med. 362, 329–344.
Reig, R., Mattia, M., Compte, A., Belmonte, C., Sanchez-Vives, M.V., 2010. Temperature modulation of slow and fast cortical rhythms. J. Neurophysiol. 103, 1253–1261.
Roopun, A.K., Middleton, S.J., Cunningham, M.O., LeBeau, F.E., Bibbig, A., Whittington, M.A., Traub, R.D., 2006. A beta2-frequency (20-30 Hz) oscillation in nonsynaptic networks of somatosensory cortex. Proc. Natl. Acad. Sci. U. S. A. 103, 15646–15650.
Ruiz-Mejias, M., Ciria-Suarez, L., Mattia, M., Sanchez-Vives, M.V., 2011. Slow and fast rhythms generated in the cerebral cortex of the anesthetized mouse. J. Neurophysiol. 106, 2910–2921.
Ruiz-Mejias, M., Martinez de Lagran, M., Mattia, M., Castano-Prat, P., Perez-Mendez, L., Ciria-Suarez, L., Gener, T., Sancristobal, B., Garcia-Ojalvo, J., Gruart, A., Delgado-Garcia, J.M., Sanchez-Vives, M.V., Dierssen, M., 2016. Overexpression of Dyrk1A, a Down syndrome candidate, decreases excitability and impairs gamma oscillations in the prefrontal cortex. J. Neurosci. 36, 3648–3659.
Sanchez-Vives, M.V., Mattia, M., 2014. Slow wave activity as the default mode of the cerebral cortex. Arch. Ital. Biol. 152, 147–155.
Sanchez-Vives, M.V., McCormick, D.A., 2000. Cellular and network mechanisms of rhythmic recurrent activity in neocortex. Nat. Neurosci. 3, 1027–1034.
Sanchez-Vives, M.V., Mattia, M., Compte, A., Perez-Zabalza, M., Winograd, M., Descalzo, V.F., Reig, R., 2010. Inhibitory modulation of cortical up states. J. Neurophysiol. 104, 1314–1324.
Sanchez-Vives, M.V., Massimini, M., Mattia, M., 2017. Shaping the default activity pattern of the cortical network. Neuron 94, 993–1001.
Shu, Y., Hasenstaub, A., McCormick, D.A., 2003. Turning on and off recurrent balanced cortical activity. Nature 423, 288–293.
Siegel, M., Donner, T.H., Engel, A.K., 2012. Spectral fingerprints of large-scale neuronal interactions. Nat. Rev. Neurosci. 13, 121–134.
Sloan, E.P., Fenton, G.W., Kennedy, N.S., MacLennan, J.M., 1995. Electroencephalography and single photon emission computed tomography in dementia: a comparative study. Psychol. Med. 25, 631–638.
Squirrell, D., 2015. An in Vivo Electrophysiological and Computational Analysis of Hippocampal Synaptic Changes in the Alzheimer's Disease Mouse. The University of Manchester, Manchester, UK.
Steriade, M., Timofeev, I., 2003. Neuronal plasticity in thalamocortical networks during sleep and waking oscillations. Neuron 37, 563–576.
Steriade, M., Nunez, A., Amzica, F., 1993. A novel slow (< 1 Hz) oscillation of neocortical neurons in vivo: depolarizing and hyperpolarizing components. J. Neurosci. 13, 3252–3265.
Steriade, M., Amzica, F., Contreras, D., 1996. Synchronization of fast (30-40 Hz) spontaneous cortical rhythms during brain activation. J. Neurosci. 16, 392–417.
Sy, M., Kitazawa, M., LaFerla, F.M., 2011. The 3xTg-AD mouse model: reproducing and modulating plaque and tangle pathology. In: Peter Paul De Deyn, D.V.D. (Ed.), Animal Models of Dementia. Springer, pp. 469–482.
Wang, X.J., 2010. Neurophysiological and computational principles of cortical rhythms in cognition. Physiol. Rev. 90, 1195–1268.
Wong, P.C., Cai, H., Borchelt, D.R., Price, D.L., 2002. Genetically engineered mouse models of neurodegenerative diseases. Nat. Neurosci. 5, 633–639.
Zucca, S., D'Urso, G., Pasquale, V., Vecchia, D., Pica, G., Bovetti, S., Moretti, C., Varani, S., Molano-Mazón, M., Chiappalone, M., Panzeri, S., Fellin, T., 2017. An inhibitory gate for state transition in cortex. Elife 6.